Mechanism and Kinetics of the Reaction between HS and Cl Radicals

Stella M. Resende and Fernando R. Ornellas*

Instituto de Química, Departamento de Química Fundamental, Universidade de São Paulo,
Caixa Postal 26077, São Paulo, SP, 05513-970, BRASIL

Received: May 11, 2000; In Final Form: September 29, 2000

The atmospheric reaction between HS and chlorine radicals was studied theoretically, using ab initio methods. We investigated three reaction possibilities: HSCl formation, and the production of HCl and sulfur, singlet and triplet. The channels that lead to HSCl and to HCl and $S(^3P)$ are spontaneous and exothermic at 298.15 K, and the channel for HCl and $S(^1D)$ formation is nonspontaneous and endothermic. In a microcanonical kinetics calculation, the rate constant we obtained for HSCl formation was 2.4×10^{-11} cm^3 molecule^{-1} s^{-1} at a pressure of 1 atm, and 2.4×10^{-13} cm^3 molecule^{-1} s^{-1} at a pressure of 0.01 atm. The rate constant for HCl and triplet sulfur production was not significantly pressure-dependent, and its value was 9.0×10^{-11} cm^3 molecule^{-1} s^{-1}. In the troposphere, the proportion of reaction products predicted was 79% for HCl and $S(^3P)$, and 21% for the formation of HSCl. At lower pressures, the proportion of HSCl decreased, and at a pressure of 0.01 atm it was predicted to be practically null. The rate constant for the total reaction was determined to be 1.1×10^{-10} cm^3 molecule^{-1} s^{-1} at 1 atm. At a pressure of 0.01 atm, this value decreased to 9.0×10^{-11} cm^3 molecule^{-1} s^{-1}, which is within the limit error of the only experimental result known in the literature.

1. Introduction

The HS radical is an important intermediate in the atmospheric chemistry of hydrogen sulfide, which is one of the reduced sulfur compounds released in great quantity in the environment.[1,2] It was believed that almost all HS generated in the atmospheric decomposition of H_2S is oxidized to SO_2 in the troposphere by common tropospheric oxidants such as O_3, NO_2, and O_2.[1,2] However, in nonpolluted areas where the concentrations of these oxidants are small, as in the remote marine boundary layer, the concentration of chlorine atoms should be sufficient[3] for the reaction with the radical HS to occur to a significant extent, leading to a coupling of the sulfur−chlorine chemistries. On the other hand, it is possible that large amounts of H_2S can also be injected in the stratosphere by volcanic eruptions,[4] leading to the production of HS in that region. Again, a coupling of the chlorine and sulfur chemistries becomes a possibility because of the presence of Cl_2 and Cl radicals in abundance in the stratosphere. It could also occur in extraterrestrial atmospheres where H_2S is abundant, as in that of Venus.[5] In general, one can expect that, if the occurrence of a coupling of the chlorine and sulfur chemistries is significant, new studies and models of the sulfur and chlorine atmospheric cycles will certainly be called for.

Despite the potential relevance of this process, to the best of our knowledge, investigations of this possibility are scarce, with reports being mainly experimental. There are studies of the reaction of chlorine atoms with other sulfur compounds such as H_2S, CH_3SH, CH_3SCH_3, and CS_2,[6,7] but the reaction with HS has not been investigated yet. The reaction between HS and Cl_2 was the subject of a recent theoretical study in our group,[8] the results showing that it is very fast and is expected to occur essentially at every encounter of the two species. The electronic structure and the photodissociation of the main product, HSCl, also was investigated,[9,10] and the results show that it will be photolyzed by sunlight, indicating that, if it is produced in the stratosphere during the polar winter, this compound should act as a temporary reservoir of chlorine.

There are some experimental measurements for the reaction between HS and the Cl radical.[11−13] Nesbitt and Leone[11] analyzed a laser-induced chemical chain reaction of the Cl_2/H_2S system, but the kinetics of the HS + Cl reaction was not determined. Clyne et al.[12] studied this reaction in a discharge-flow system linked to a quadrupole mass spectrometer. They observed the formation of a yellow deposit on the walls, which was attributed to sulfur formation. Monitoring the HS peak, the ratio between the rate constants of the HS + Cl and the H_2S + Cl reactions was measured, and the rate constant of the reaction between HS and Cl was determined as $(1.1 \pm 0.3) \times 10^{-10}$ cm^3 molecule^{-1} s^{-1}. Eberhard et al.,[13] using a discharge-flow reactor coupled with a photoionization mass spectrometer, have also identified a sulfur yellow deposit. All of these studies were conducted in low-pressure conditions, and it was believed that the reaction would lead to the abstraction products, HCl and S. However, in the troposphere, another channel should be possible, which will lead to the addition product. In view of the facts above, the main purpose of this work is to investigate the mechanism and the kinetics of the reaction between HS and chlorine atom, leading to other possible pathways, at different atmospheric conditions. It is our hope that it can contribute further to a better understanding of the chlorine and sulfur chemistries in the atmosphere.

2. Methodology and Calculation

A. Potential Energy Surface. Considering the two possible spin states for the sulfur radical, three channels should be considered:

10.1021/jp001751q CCC: $19.00

$$\mathrm{HS} + \mathrm{Cl} \rightarrow \mathrm{HSCl} \quad (1)$$

$$\mathrm{HS} + \mathrm{Cl} \rightarrow \mathrm{HCl} + \mathrm{S}\ (^1\mathrm{D}) \quad (2)$$

$$\mathrm{HS} + \mathrm{Cl} \rightarrow \mathrm{HCl} + \mathrm{S}\ (^3\mathrm{P}) \quad (3)$$

The channel that leads to the addition product, HSCl, does not have a potential energy barrier. The minimum energy reaction path was constructed following the S—Cl coordinate and optimizing the other variables. The optimizations were performed with the GAMESS package,[14] using the cc-pVTZ basis set at the CASSCF level of theory. The active space included the valence orbitals of the three atoms. Next, the effect of dynamical correlation was included through a multireference configuration interaction (MRCI) calculation, using the Molpro package.[15] The orbitals used in the MRCI step were generated from a state-averaged CASSCF/cc-pVQZ calculation, including three states of A' symmetry in the C_s group point with the active space now restricted to the four nonfully occupied orbitals because of convergence problems at large intermolecular distances. In the MRCI step, a new reference set, which included all configuration state functions with coefficients greater than 0.025 in magnitude was constructed. The final CI wave function consisted of all single and double excitations from this new reference set. This restriction allows us to limit the length of the CI expansion to a manageable size.

The optimization of stationary points for channels 2 and 3 were also performed at the same level of theory, a CASSCF calculation with the cc-pVTZ basis set. Because the multiconfigurational character was small in all stationary points investigated, MP2 and CCSD(T) single-point calculations were performed to assess the dynamical electronic correlation effects. These latter calculations were performed with the Gaussian package.[16] The procedure developed by Dunning and coworkers[17] to reach basis set completeness was used, and the additivity approximation[18,19] also included to obtain values for the complete basis set (CBS) limit at the CCSD(T) level of correlation. This procedure has already been used in a previous calculation and the results have been reliable.[8] The energy of the singlet sulfur was obtained in the same manner as that of the triplet plus the singlet—triplet energy gap, calculated at the MRCI level. In this step, the reference set of molecular orbitals was generated from a CASSCF calculation performed with the aug-cc-pVQZ basis set, and having the 3s and 3p orbitals as the active space.

Channel 2 is expected to occur in two steps: formation of HSCl, followed by its decomposition to HCl and S(^{1}D), as presented below.

$$\mathrm{HS} + \mathrm{Cl} \rightarrow \mathrm{HSCl} \quad (2a)$$

$$\mathrm{HSCl} \rightarrow \mathrm{HCl} + \mathrm{S}(^1\mathrm{D}) \quad (2b)$$

In channel 3, which leads to the triplet state of sulfur, it will proceed through the formation of a triplet weakly bound complex, which will lead to the products, HCl and S(^{3}P). This reaction path can be described as:

$$\mathrm{HS} + \mathrm{Cl} \rightarrow \mathrm{HS}\cdots\mathrm{Cl} \quad (3a)$$

$$\mathrm{HS}\cdots\mathrm{Cl} \rightarrow \mathrm{HCl} + \mathrm{S}(^3\mathrm{P}) \quad (3b)$$

The step that leads to the formation of the weakly bound complex (3a) also occurs without a potential energy barrier. Its reaction path was constructed following the S—Cl distance, with the H—S distance fixed at 1.3391 Å and the Cl—H—S angle at 45.0 degrees. This procedure is justified in this case because it represents a very weak bond, and the intramolecular distance HS and the intermolecular angle will not be modified significantly in the reaction path. The multiconfigurational character is negligible, and the same procedure used earlier to reach basis set completeness and a higher level of electronic correlation description was also applied for this step.

B. Kinetic Model. All channels for this reaction system begin with a bimolecular collision between the HS and Cl radicals. They will lead to the activated HSCl and HS···Cl species, which can be deactivated or react, backward or forward, resulting in new products. Because this reaction system does not involve complex species, there will be few vibrational states available for energy distribution. Consequently, the concentration of energy in the internal mode responsible for the reaction will be very effective and the reaction will proceed very quickly. In this case, once the first step occurs, the next one will be faster than the product deactivation through collision with another species, and a microcanonical treatment is needed to determine these rate constants. Consequently, rate constants were calculated using RRKM theory for unimolecular reactions.[20] Within this approach, the rate constant will be given as the ratio between the sum of states for the active degrees of freedom in the critical configuration, which is the transition state, with total energy E, $G(E)$, and the density of states for the active degrees of freedom in the reactants, $N(E)$:

$$k_{\mathrm{a}}(E) = \frac{G(E^{\neq})}{hN(E)} \quad (1)$$

This equation was implemented in the RRKM program developed by Zhu and Hase,[21] and was used to calculate microcanonical rate constants for the reactions steps above, assuming $J = 0$.

Thermodynamic properties, such as Gibbs free energy and enthalpy, were calculated for all reaction steps. We have used harmonic frequencies and geometrical parameters obtained in the optimization at the CASSCF level of theory.

Rate constants for steps 2a and 3a have also been calculated using transition state theory (TST)[22] to determine the high-pressure limit for these quantities. In the transition state for the weakly bound complex formation, the harmonic analysis of the vibrational frequencies is not suitable, and a value for the nuclear contribution to the Gibbs free energy was estimated by use of the collision rate approximation. The values were calculated considering the HS···Cl system as a pseudo-diatomic molecule, with a variable HS—Cl distance. In all kinetic calculations we considered a temperature of 298.15 K and pressures of 1 and 0.01 atm. These conditions allowed us to obtain values corresponding to reactions in the troposphere and stratosphere and to compare our kinetic results with existing experimental ones.

3. Results and Discussion

A. Reaction Mechanism. We will first focus on the description of the activation properties of channel 1 (step 2a) and step 3a, which are the reactions that do not have an activation potential energy barrier. For step 2a, the variation in the potential energy and the Gibbs free energy, as a function of the S—Cl distance, calculated at the MRCI/cc-pVQZ level of theory is represented in Figure 1. The maximum of the Gibbs free energy curve corresponds to a geometry where the S—Cl distance is 4.0 Å. It is the variational transition state structure for this step and is labeled TS1. The activation Gibbs free energy for this

TABLE 1: Calculated Energies (in Hartree), Zero-Point Energies (ZPE, in kcal/mol) and CI Coefficients for the Zero-Order Function[a]

	CASSCF/cc-pVTZ	ZPE	CI coef.	PMP2/aug-cc-pVDZ	PMP2/aug-cc-pVTZ	PMP2/aug-cc-pVQZ	CCSD(T)/aug-cc-pVTZ	MRCI aug-cc-pVQZ
HS	−398.11856	3.675	0.99	−398.21392	−398.26246	−398.27784	−398.29129	–
Cl	−459.47995	0.000	0.98	−459.59353	−459.64932	−459.66769	−459.67622	–
HSCl	−857.67591	5.677	0.98	−857.89493	−858.01186	−858.05017	−858.06467	–
TS3	−857.58395	2.054	0.94	−857.81049	−857.91478	−857.94897	−857.97257	–
HS···Cl	−857.60143	4.469	0.90	−857.82509	−857.92999	−857.96481	−857.98743	–
HCl	−460.12457	4.185	0.99	−460.25182	−460.31504	−460.33599	−460.34320	–
S(^{3}P)	−397.50597	0.000	1.00	–	–	–	–	−397.65658
S(^{1}D)	−397.45307	0.000	1.00	–	–	–	–	−397.61377

[a] The optimizations were performed at the CASSCF level of theory, with the cc-pVTZ basis set.

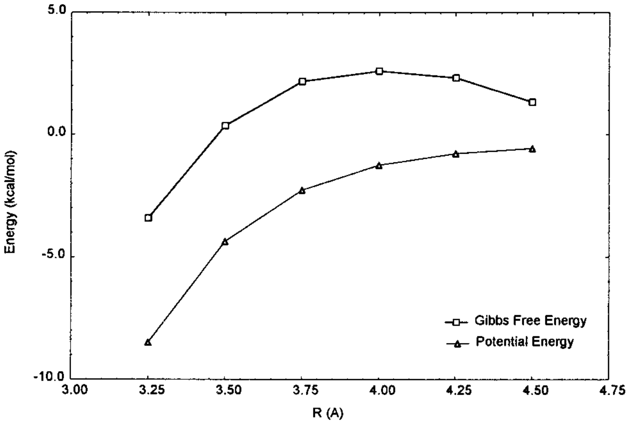

Figure 1. Potential energy surface for the HS + Cl reaction, leading to the HSCl product. R is S—Cl the distance.

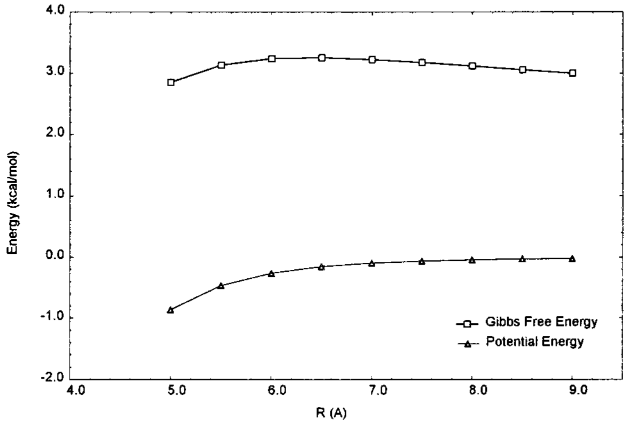

Figure 2. Potential energy surface for the HS + Cl reaction, leading to the HS···Cl weakly bound complex. R is the S—Cl distance.

channel amounts to 2.60 kcal/mol, and when spin degeneracy is taken into account, it increases to 3.42 kcal/mol.

In step 3a, the curves for the variation of the potential energy and the Gibbs free energy with the distance S—Cl are depicted in Figure 2. The maximum in the curve will occur at a distance of 6.5 Å, resulting in an activation Gibbs free energy for this step of 3.42 kcal/mol, including the spin degeneracy contribution. This point is labeled TS2.

For step 3b, a transition state was obtained (TS3), and the reaction path was confirmed through an intrinsic reaction coordinate (IRC) calculation. Energy values for this stationary point and for other species participating of this reaction are collected in Table 1. The optimization process was performed at the CASSCF/cc-pVTZ level of theory, and additional calculations at these geometries with different methodological approaches are also presented in this table. Geometric representations of these points and of TS1 along with the more relevant geometrical parameters are shown in Figure 3. For all stationary points, the CI coefficient of the zero-order function is ≥0.90.

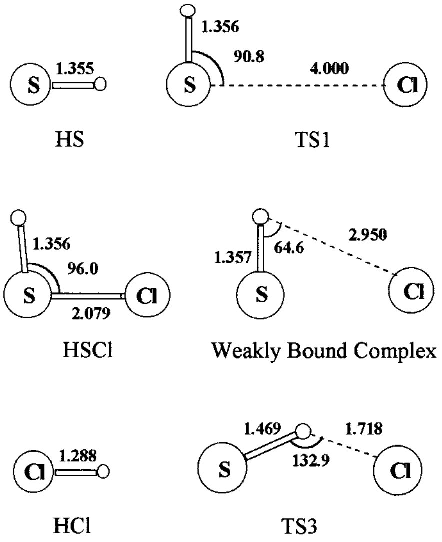

Figure 3. Schematic representation along with the relevant geometrical parameters of all stationary points obtained in the study of the reaction between HS and Cl, at the CASSCF level of calculation with the cc-pVTZ basis set.

TABLE 2: Harmonic Frequencies (in cm^{-1}) for HSCl and HS···Cl Species at the CASSCF/cc-pVTZ Level of Optimization

assignment	HSCl	HS···Cl
H—S stretching	2565.85	2601.05
bending	899.51	379.30[a]
S—Cl stretching	505.48	
HS···Cl stretching		145.83[a]

[a] Intermolecular modes.

Relative energies and thermodynamic properties for the activation and the reaction itself of all reaction steps investigated are shown in Table 3 and Table 4, respectively, at different levels of theory. Figure 4 depicts a profile of the potential energy surface for the overall reaction, and Figure 5 shows the corresponding variation of the Gibbs free energy. From these tables, we see a small and nonsignificant variation in the results with the basis set size, indicating that the basis set limit was reached, whereas at the three levels of electronic correlation considered, CASSCF, MP2, and CCSD(T), the results differ by a few kilocalories.

Focusing our attention on the different channels, we can say that, in channel 1, the formation of HSCl is very favorable thermodynamically. At the CCSD(T)/CBS level of theory, the reaction Gibbs free energy and the enthalpy of reaction are

TABLE 3: Thermodynamic Activation Properties (in kcal/mol, Standard State 1 atm Pressure) of the Reaction Steps Studied

	CASSCF/cc-pVTZ	PMP2/aug-cc-pVTZ	PMP2/aug-cc-pVQZ	PMP2/CBS	CCSD(T)/ aug-cc-pVTZ	CCSD(T)/ aug-cc-pVQZ	CCSD(T)/CBS
			reaction 2a				
ΔE^a	−0.49	–	–	–	–	–	-1.16^b
ΔH	−1.17	–	–	–	–	–	-1.84^b
ΔG	4.09	–	–	–	–	–	3.42^b
			reaction 3a				
ΔG	–	3.31	3.31	3.32	3.24	3.25	3.42
			reaction 3b				
ΔE	8.55	7.13	7.53	7.92	6.91	7.31	7.71
ΔH	8.34	6.92	7.31	7.71	6.70	7.10	7.50
ΔG	9.04	7.61	8.01	8.40	7.39	7.79	8.19

[a] Activation energy, which corresponds to the classical activation energy plus the ZPE contribution. [b] MRCI/cc-pVQZ results.

TABLE 4: Thermodynamic Reaction Properties (in kcal/mol, Standard State 1 atm Pressure) of the Reaction Steps Studied

	CASSCF/cc-pVTZ	PMP2/aug-cc-pVTZ	PMP2/aug-cc-pVQZ	PMP2/CBS	CCSD(T)/ aug-cc-pVTZ	CCSD(T)/ aug-cc-pVQZ	CCSD(T)/CBS
			reaction 2a				
ΔE^a	−46.57	−60.88	−63.67	−65.25	−58.96	−61.75	−63.45
ΔH	−47.58	−61.89	−64.68	−66.26	−59.97	−62.77	−64.46
ΔG	−41.31	−55.61	−58.40	−59.99	−53.70	−56.49	−57.37
			reaction 2b				
ΔE^a	60.17	–	–	–	–	–	71.09^b
ΔH	61.18	–	–	–	–	–	72.10^b
ΔG	54.97	–	–	–	–	–	65.89^b
			reaction 3a				
ΔE^a	−1.04	−10.70	−11.31	−11.94	−11.70	−12.31	−12.94
ΔH	−1.61	−11.27	−11.88	−12.51	−12.27	−12.88	−13.50
ΔG	3.49	−6.18	−6.78	−7.41	−7.18	−7.78	−8.24
			reaction 3b				
ΔE^a	−17.15	−9.65	−8.88	−21.01	−7.76	−6.99	−6.29
ΔH	−16.58	−9.08	−8.31	−20.44	−7.19	−6.42	−5.72
ΔG	−21.61	−14.11	−13.34	−25.47	−12.22	−11.45	−10.75

[a] Reaction energy, which corresponds to the classical reaction energy plus the ZPE contribution. [b] MRCI/aug-cc-pVQZ results.

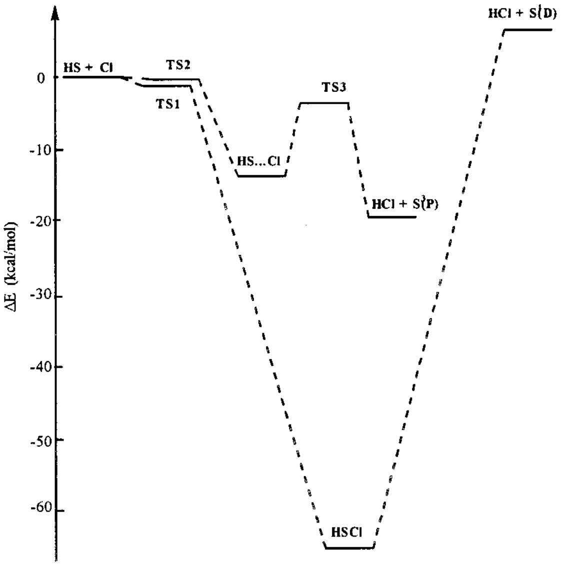

Figure 4. Energy diagram for the HS−Cl reaction, at our best level of calculation, CCSD(T)/CBS. Exception is the TS1 profile, which was obtained at the MRCI/cc-pVQZ level of theory.

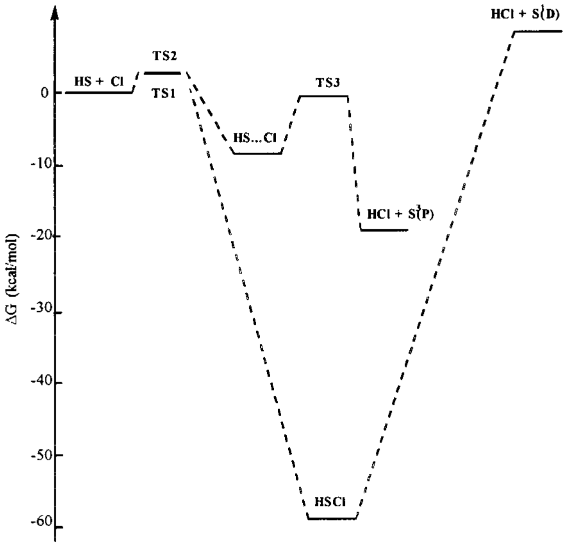

Figure 5. Gibbs free energy diagram for the HS−Cl reaction, at our best level of calculation, CCSD(T)/CBS. Exception is the TS1 profile, which was obtained at the MRCI/cc-pVQZ level of theory.

−57.37 and −64.46 kcal/mol, respectively. The enthalpy value reported in a previous work, −62 kcal/mol,[11] is in reasonable agreement with the present results.

For channel 2, leading to the production of sulfur in the singlet state, but passing by the formation of the HSCl molecule, the singlet−triplet energy gap calculated in this work, 26.86 kcal/mol, is in excellent agreement with the experimental value of 26.41 kcal/mol.[23] However, step 2b, which involves the production of HCl and S(^{1}D) from HSCl, has a reaction Gibbs free energy of 65.89 kcal/mol and is endothermic by 72.10 kcal/mol. Because this process is not spontaneous, the kinetic properties were not calculated. With respect to the reactants HS and Cl, the change of Gibbs free energy and enthalpy is 8.52 and 7.64 kcal/mol, respectively.

TABLE 5: Calculated Rate Constants for All Steps of Channels 2 and 3 for the Reaction between HS and Cl

reaction	k	method
2a	7.86×10^{-10} cm^3 molecule^{-1} s^{-1}	TST
−2a	1.13×10^{12} s^{-1}	RRKM
3a	7.86×10^{-10} cm^3 molecule^{-1} s^{-1}	TST
−3a	3.19×10^{13} s^{-1}	RRKM
3b	4.12×10^{12} s^{-1}	RRKM

SCHEME 1

In channel 3, which leads to a sulfur atom in a triplet state, the first step involves the formation of a weakly bound complex between HS and Cl. The next step occurs through the transition state TS3, which finally leads to the products, HCl and S(^{3}P). The HS···Cl complex is not so stable as HSCl, but the transition state for its dissociation is energetically very close to the reactant energy level. The thermodynamic properties for this channel, Gibbs free energy and enthalpy of reaction, are −18.99 kcal/mol and −19.22 kcal/mol, respectively. The value obtained for the enthalpy of reaction is in very good agreement with the result of −18.1 kcal/mol reported previously.[12]

B. Calculation of the Rate Constants. The calculated rate constants for all reaction steps considered in this work are presented in Table 5, where the method used is also indicated. To perform a kinetic analysis of the total reaction, the channels with different multiplicities have been treated separately. In a microcanonical situation, once channel 1 (or the first step of channel 2) is followed, the HSCl formed is activated (HSCl*). There are two possible fates for HSCl: deactivation, loosing energy to the walls or another species (reaction c), or dissociation (inverse reaction), producing HS and Cl again (reaction −a), as shown in Scheme 1.

Considering the steady-state approximation and supposing that the deactivation of HSCl* will proceed at the collision rate, k_{col}, we can obtain, for the rate of change of HSCl concentration, the expression

$$\frac{\mathrm{d}[\mathrm{HSCl}]}{\mathrm{d}t} = k_{\mathrm{cl}}[\mathrm{M}][\mathrm{HSCl}^*] = \frac{k_{2\mathrm{a}}k_{\mathrm{col}}[\mathrm{M}][\mathrm{HS}][\mathrm{Cl}]}{k_{-2\mathrm{a}} + k_{\mathrm{col}}[\mathrm{M}]} \tag{2}$$

In this equation, all rate constants are energy-dependent. However, we can suppose that the energy distribution will be concentrated in an average value, which is the thermal energy of the reactants. Therefore, the rate constant for channel 1 can be given as

$$k_1 = \frac{k_{2\mathrm{a}}k_{\mathrm{col}}[\mathrm{M}]}{k_{-2\mathrm{a}} + k_{\mathrm{col}}[\mathrm{M}]} \tag{3}$$

where all rate constants are calculated at the thermal energy of the reactants. The rate constant for the bimolecular step (2a) was obtained from a TST calculation, because in this case the system is thermally equilibrated. To evaluate the collision rate constant, we considered helium as the inert gas, as in the experimental conditions, and the distance of collision as being 5 Å, which leads to a value for k_{col} of 1.42×10^{-9} cm^3 s^{-1}. At a pressure of 1 atm, the rate constant for channel 1 is 2.35×10^{-11} cm^3 molecule^{-1} s^{-1}, whereas it is 2.43×10^{-13} cm^3 molecule^{-1} s^{-1} at a pressure of 0.01 atm. As we have already discussed, step 2b of Channel 2 will not occur because it is not spontaneous.

SCHEME 2

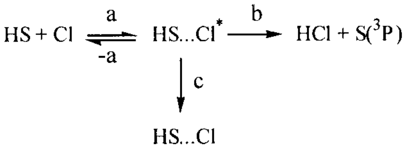

A similar picture can also be considered for channel 3, as presented in Scheme 2, and equivalent calculations can be performed. The kinetic equation can be expressed by

$$k_3 = \frac{k_{3\mathrm{a}}k_{3\mathrm{b}}}{k_{-3\mathrm{a}} + k_{3\mathrm{b}} + k_{\mathrm{col}}[\mathrm{M}]} \tag{4}$$

The kinetic results are 8.98×10^{-11} cm^3 molecule^{-1} s^{-1} at a pressure of 1 atm and 8.99×10^{-11} cm^3 molecule^{-1} s^{-1} at a pressure of 0.01 atm.

This reaction is controlled by the kinetics and the product proportion among these three channels can be obtained by the kinetic rate constants. It will lead to a proportion of 21% of HSCl production (channel 1) and 79% of the triplet pathway (channel 3) at 1 atm. At low pressures, the dissociation products will be favored, and at 0.01 atm, channel 1 will not occur, and the only products will be HCl and S(^{3}P). These findings are in agreement with the conclusions of Eberhard et al.,[13] who stated that the HSCl observed in their experiment in a very low pressure should be produced by a parallel reaction between HS and Cl_2.

Adding the two channels, a total rate constant for the reaction of HCl and sulfur production can be obtained, being $k_{\mathrm{obs}}(1\ \mathrm{atm}) = 1.13 \times 10^{-10}$ cm^3 molecule^{-1} s^{-1} and $k_{\mathrm{obs}}(0.01\ \mathrm{atm}) = 9.01 \times 10^{-11}$ cm^3 molecule^{-1} s^{-1}. For the only experimental result available, $(1.1 \pm 0.3) \times 10^{-10}$ cm^3 molecule^{-1} s^{-1},[12] our result is within the experimental error. In fact, these two values are in excellent agreement.

C. Atmospheric Implications. Our results show that the reaction between HS and Cl will be very fast, with a small pressure dependence, showing that a coupling of the sulfur and chlorine chemistry is possible in the troposphere and stratosphere (low-pressure conditions). In the troposphere, the channels leading to HSCl and to HCl + S(^{3}P) formation will occur, but a preference to HCl and S(^{3}P) production has been derived from our results. At lower pressures, the proportion of HCl and S(^{3}P) formation relative to HSCl formation will increase, and at 0.01 atm, only HCl and S(^{3}P) will be produced. To assess the tropospheric role of this reaction, an average atmospheric concentration of the HS radical should be obtained. Using the rate constants[1] and typical atmospheric concentrations of O_3 and NO_2,[24] a lifetime of 0.3 s can be estimated for the HS radical. Assuming a concentration of H_2S of 2 parts per trillion by volume (pptv) in the boundary marine layer,[2] the steady-state concentration of HS can be obtained as being ca. 4×10^4 molecule cm^3, which will lead to a lifetime of chlorine of 3 days, using the kinetic constant determined in this work. So, it will not play an important role in the atmospheric concentration of the chlorine atoms in the troposphere. On the other hand, in the stratosphere, the importance of this reaction will be conditioned by the presence of HS radical in this region, which is due to volcanic eruptions. Therefore, because HS occurrence in the stratosphere will somehow be instantaneous, a reliable value of this concentration is usually not well-known. However, the chlorine concentration is almost 4 ppb,[25] and our results indicate that the reaction of HS with chlorine should occur in a significant extension in this situation. In fact, in the stratosphere, the lifetime of HS relative to the reaction with chlorine will be 0.1 s, which can be significant when compared with the lifetime of HS with O_3 in this region. Therefore, this reaction could act minimizing the destructive potential of the reaction HS + O_3 to the ozone layer. Also, considering the catalytic behavior of the chlorine radicals to the ozone layer destruction, this reaction could act as an additional means of capturing chlorine radicals and transforming them into a more stable molecule, HCl. These possibilities, however, should be investigated further together with other sulfur compound reactions to have a better assessment of their importance in the ozone hole formation.

4. Conclusions

In this work, the kinetics and mechanism of the reaction between HS and chlorine radicals was studied theoretically by high-level ab initio calculations, and TST and RRKM kinetic theories. Our results show that two channels are possible: one that leads to the HSCl molecule, and another that leads to the products HCl and S(^{3}P). The formation of HSCl occurs without a potential energy barrier. The production of the HCl and S(^{3}P) involves the formation of a weakly bound complex, and this reaction also does not have a potential energy barrier in the first step. The rate constants for all steps were calculated, and the total reaction is expected to be very fast, with a predominance of the products HCl and S(^{3}P). The formation of HSCl is predicted to occur only at high pressures. Our kinetic value is in excellent agreement with the only experimental result available. In the stratosphere, if the HS concentration reaches a significant value, a likely event after a strong volcanic eruption, it will react with chlorine radicals, transforming it in a less reactive molecule, HCl. Also, the reaction HS + Cl may become competitive with the ozone layer destructive reaction HS + O_3, making this latter process to occur in a smaller extension under that condition.

Acknowledgment. The authors are grateful to Fundação de Amparo à Pesquisa do Estado de São Paulo (FAPESP) for the academic support (grants no. 99/02963-1 and 99/02962-5), and to Laboratório de Computação Científica Avançada (LCCA/USP) for the computational resources. Helpful discussions with Dr. Josefredo R. Pliego Jr. are also acknowledged. F.R.O. also thanks the Conselho Nacional de Desenvolvimento Científico e Tecnológico (CNPq).

References and Notes

(1) Tyndall, G. S.; Ravishankara, A. R. *Atmos. Environ., Part A* **1991**, *23*, 483.

(2) Wilson, C.; Hirst, D. M. *Prog. React. Kinet.* **1996**, *21*, 69.

(3) Vogt, R.; Crutzen, P. J.; Sander, R. *Nature* **1996**, *383*, 327.

(4) Kotra, J. P.; Finnegan, D. L.; Zoller, W. H.; Hart, M. A.; Moyers, J. L. *Science* **1983**, *222*, 1018.

(5) Eibling, R. E.; Kaufman, M. *Atmos. Environ., Part A* **1983**, *17*, 429.

(6) Wilson, C.; Hirst, D. M. *J. Chem. Soc., Faraday Trans.* **1997**, *93*, 2831.

(7) Resende, S. M.; De Almeida, W. B. *J. Phys. Chem. A* **1997**, *101*, 9738.

(8) Resende, S. M.; Ornellas, F. O. *Chem. Phys. Lett.* **2000**, *318*, 340.

(9) Ornellas, F. R. *Theor. Chem. Acc.* **2000**, *103*, 469.

(10) Ornellas, F. R.; Resende, S. M. *J. Phys. B: At. Mol. Opt. Phys.* **2000**, *33*, L383.

(11) Nesbitt, D. J.; Leone, S. R. *J. Chem. Phys.* **1980**, *72*, 1722.

(12) Clyne, M. A. A.; MacRobert, A. J.; Murrels, T. P.; Stief, L. J. *J. Chem. Soc., Faraday Trans.* **1984**, *80*, 877.

(13) Eberhard, J.; Chen, W.-C.; Yu, C.-H.; Lee, Y.-P.; Cheng, B.-M. *J. Chem. Phys.* **1998**, *108*, 6197.

(14) Schmidt, M. W.; Baldridge, K. K.; Boatz, J. A.; Elbert, S. T.; Gordon, M. S.; Jensen, J. H.; Koseki, S.; Matsunaga, N.; Nguyen, K. A.; Su, S.; Windus, T. L.; Dupuis, M.; Montgomery, J. A. *J. Comput. Chem.* **1993**, *14*, 1347.

(15) MOLPRO is a package of ab initio programs written by Werner, H. J. and Knowles, P. J.; with contributions from Almlöf, J.; Amos, R. D.; Berning, D. L.; Cooper, M. J. O.; Deegan, M. J. O.; Dobbyn, A. J.; Eckert, F.; Elbert, S. T.; Hampel, C.; Lyndh, R.; Lloyd, A. W.; Meyer, W.; Nicklass, A.; Peterson, K.; Pitzer, R.; Stone, A. J.; Taylor, P. R.; Mura, M. E.; Pulay, P.; Schütz, M.; Stoll, H.; Thorsteinsson, T.

(16) Frisch, M. J.; Trucks, G. W.; Schlegel, H. B.; Gill, P. M. W.; Johnson, B. G.; Robb, M. A.; Cheeseman, J. R.; Keith, T.; Petersson, G. A.; Montgomery, J. A.; Raghavachari, K.; Al-Laham, M. A.; Zakrzewski, V. G.; Ortiz, J. V.; Foresman, J. B.; Cioslowski, J.; Stefanov, B. B.; Nanayakkara, A.; Challacombe, M.; Peng, C. Y.; Ayala, P. Y.; Chen, W.; Wong, M. W.; Andres, J. L.; Replogle, E. S.; Gomperts, R.; Martin, R. L.; Fox, D. J.; Binkley, J. S.; Defrees, D. J.; Baker, J.; Stewart, J. P.; Head-Gordon, M.; Gonzalez, C.; Pople, J. A. *Gaussian 98*, Revision D.2; Gaussian, Inc.: Pittsburgh, PA, 1998.

(17) Woon, D. E.; Dunning, T. H. *J. Chem. Phys.* **1993**, *99*, 1914.

(18) Curtiss, L. A.; Raghavachari, K.; Trucks, G. W.; Pople, J. A. *J. Chem. Phys.* **1991**, *94*, 7221.

(19) Nobes, R. H.; Bouma, W. J.; Radom, L. *Chem. Phys. Lett.* **1982**, *89*, 497.

(20) Holbrook, K. A.; Pilling, M. J.; Robertson, S. H. *Unimolecular Reactions*; Wiley: England, 1996.

(21) Zhu, L.; Hase, W. L. A General RRKM Program which is a modification of the Hase/Bunker RRKM Program, QCPE 234, Department of Chemistry, Wayne State University, 1994.

(22) Steinfeld, J. L.; Francisco, J. S.; Hase, W. L. *Chemical Kinetics and Dynamics*; Prentice Hall: New York, 1989.

(23) Radzig, A. A.; Smirnov, B. M. *Reference Data on Atoms, Molecules and Ions*; Springer-Verlag: Berlin, 1985.

(24) Wang, N. S.; Howard, C. J. *J. Phys. Chem.* **1990**, *94*, 8787.

(25) Rowland, F. S. *Annu. Rev. Phys. Chem.* **1991**, *42*, 731.